HHS Public Access

Author manuscript

Mol Cell Endocrinol. Author manuscript; available in PMC 2019 February 05.

Published in final edited form as:

Mol Cell Endocrinol. 2018 February 05; 461: 22–31. doi:10.1016/j.mce.2017.08.005.

Deletion of Protein Kinase D1 in Osteoprogenitor Cells Results in Decreased Osteogenesis *in vitro* and Reduced Bone Mineral Density *in vivo*

Wendy B. Bollag[1,2,3,4,5,#], **Vivek Choudhary**[1,3], **Qing Zhong**[2,6], **Ke-Hong Ding**[2,6], **Jianrui Xu**[2,6], **Ranya Elsayed**[7], **Kanglun Yu**[8], **Yun Su**[2,6], **Lakiea J. Bailey**[2,6], **Xing-Ming Shi**[2,4,6], **Mohammed Elsalanty**[2,7], **Maribeth H. Johnson**[9], **Meghan E. McGee-Lawrence**[2,8], and **Carlos M. Isales**[2,4,6]

[1]Charlie Norwood VA Medical Center, Augusta, Georgia, 30904

[2]Institute for Regenerative and Reparative Medicine, Augusta University 30912

[3]Department of Physiology, Augusta University 30912

[4]Department of Orthopaedic Surgery, Augusta University 30912

[5]Department of Medicine, Augusta University 30912

[6]Department of Neuroscience and Regenerative Medicine, Augusta University 30912

[7]Department of Oral Biology, Augusta University 30912

[8]Department of Cellular Biology and Anatomy, Augusta University 30912

[9]Department of Biostatistics and Epidemiology, Augusta University 30912

Abstract

Protein kinase D1 (PRKD1) is thought to play a role in a number of cellular functions, including proliferation and differentiation. We hypothesized that PRKD1 in bone marrow-derived mesenchymal stem cells (BMMSC) could modulate osteogenesis. In BMMSCs from floxed PRKD1 mice, PRKD1 ablation with adenovirus-mediated Cre-recombinase expression inhibited BMMSC differentiation *in vitro*. In 3- and 6-month-old conditional knockout mice (cKO), in which PRKD1 was ablated in osteoprogenitor cells by osterix promoter-driven Cre-recombinase, bone mineral density (BMD) was significantly reduced compared with floxed control littermates. Microcomputed tomography analysis also demonstrated a decrease in trabecular thickness and bone volume fraction in cKO mice at these ages. Dynamic bone hisotmorphometry suggested a mineralization defect in the cKO mice. However, by 9 months of age, the bone appeared to compensate for the lack of PRKD1, and BMD was not different. Taken together, these results suggest a potentially important role for PRKD1 in bone formation.

[#]Corresponding Author: Wendy B. Bollag, Department of Physiology, Augusta University, 1120 15th Street, Augusta, GA 30912, Tele: (706) 721-0698, FAX: (706) 721-7299, wbollag@augusta.edu.

Keywords

Bone; Mesenchymal stem cells; Mineralization; Osteoprogenitor; Osterix; Protein kinase D1

1. Introduction

Bone loss results from either decreased bone formation and/or enhanced bone resorption leading to osteopenia or osteoporosis, which affects roughly 44 million Americans. Aging is associated with a gradual and progressive bone loss. Although the mechanisms that lead to reduced bone density with age are not well understood, decreased bone formation with aging plays an important role. Aging is also known to be associated with the generation of excessive reactive oxygen species (ROS), which can inhibit osteoblastic differentiation of BMMSCs and their mineralization (e.g., (Kim et al., 2010, Bai et al., 2004) and reviewed in (Hamada et al., 2009)). Importantly, differentiation of BMMSCs results in their increased use of oxidative phosphorylation for ATP production (Guntur et al., 2014); this change in cell metabolism would be expected to enhance the generation of ROS (Guntur et al., 2014). Thus, in order for osteoblastic differentiation of BMMSCs to proceed in the face of this stimulated ROS generation, these cells apparently must up-regulate mechanisms to protect themselves against this oxidative stress.

Protein kinase D (PRKD) family members have been implicated in a number of important cellular functions, such as Golgi trafficking, hypertrophy, proliferation, immune responses, migration, invasion and survival (reviewed in (Guha et al., 2010) (LaValle et al., 2010)). Recent studies also indicate a potentially important role for PRKD1 in bone physiology *in vitro* and *in vivo* (Ford et al., 2013, Yeh et al., 2010, Jensen et al., 2009). However, its exact role in the various cell types regulating bone homeostasis (e.g., mesenchymal stem cells, osteoblasts, osteoclasts and osteocytes) and the mechanism by which this kinase exerts its effects in bone are unclear.

A few studies have investigated the role of PRKD1 in bone function or the mechanisms by which it acts (Yeh et al., 2010, Jensen et al., 2009). Investigators have demonstrated *in vitro* activation of PRKD1 by bone morphogenic proteins (BMP), including BMP2 and BMP7, as well as a role for this enzyme in regulating bone cell function (Yeh et al., 2010, Jensen et al., 2009, Lemonnier et al., 2004, Celil and Campbell, 2005). *In vivo,* Ford et al. (Ford et al., 2013) used transgenic mice in which one PRKD1 allele is replaced with an inactivatable (dominant-negative) PRKD1 mutant to demonstrate a role for PRKD in pubertal bone growth. However, there are several limitations with this model: (1) only mice heterozygous for this PRKD1 mutant can be studied due to the fact that homozygosity is lethal (Ford et al., 2013), (2) the mutant is global so the observed changes in bone mineral density could not be attributed directly to effects on osteoblasts, since differences in osteoclasts were also observed (Ford et al., 2013) and (3) the inactivatable PRKD mutant used may act in a dominant-negative manner towards PRKD2 in addition to PRKD1 (Yin et al., 2008). To address these issues, in this report we made use of a floxed PRKD1 mouse model (Flelitz et al., 2008) to ablate the PRKD1 gene in bone using Cre recombinase. These studies were performed in bone marrow-derived mesenchymal stem cells (BMMSCs) *in vitro* and

osteoprogenitor cells *in vivo* by crossing PRKD1 floxed mice with the transgenic mouse in which the osterix promoter drives Cre expression (Rodda and McMahon, 2006). We then evaluated bone mineral denisty (BMD) and other key parameters in mature (3–12 months of age) conditional knockout (cKO) compared to floxed mice of various ages. Our results suggest an important role for PRKD1 in regulating bone turnover.

2. Methods

2.1. Bone Marrow-Derived Mesenchymal Stem Cell Isolation and Culture

The Augusta University Stem Cell Core Facility prepared BMMSCs from PRKD1 floxed mice as described in (Flelitz et al., 2008) from bone marrow harvested from femora of approximately 3-month-old floxed PRKD1 mice (Flelitz et al., 2008). These mice were generously provided by Dr. Eric Olson (University of Texas Southwestern Medical Center, Dallas, TX). All experiments were conducted in accordance with protocols approved by the Augusta University Institutional Animal Care and Use Committee (Protocol #BR09-11-265). Mice were euthanized by carbon dioxide overdose followed by thoracotomy, an American Veterinary Medical Association-approved method.

2.2. *In vitro* PRKD1 Gene Ablation

Isolated BMMSCs derived from PRKD1 floxed mice cells were infected with GFP-expressing (control) adenovirus and adenovirus expressing Cre recombinase (and GFP) to delete the PRKD1 gene as performed previously in epidermal keratinocytes (Choudhary et al., 2014). These cells were then cultured for 1–2 days before stimulation with the indicated reagents or transfer into an osteogenic medium as described below. In addition, BMMSCs in which PRKD1 was or was not stably ablated (via infection with Cre- or GFP-adenovirus, respectively) were passaged several times prior to plating in appropriate tissue culture dishes for experimentation.

2.3. Quantitative Reverse Transcription-Polymerase Chain Reaction (qRT-PCR)

Cells (BMMSCs infected with GFP- or Cre-adenovirus or passaged from cells) were harvested and RNA isolated using PerfectPure RNA Tissue kits (5 Prime, Gaithersburg, MD). RNA was reverse-transcribed using iScript cDNA synthesis kits (Bio-Rad, Hercules, CA) and the resultant cDNA analyzed by qRT-PCR in a 20 μL reaction volume containing Supermix and primer-probe sets obtained from Applied Biosystems (Thermo Scientific, Waltham, MA). Data were analyzed using the delta-delta-Ct method using the average Ct value for GAPDH and RPLP0 as the housekeeping genes and GFP-infected, untreated samples as the comparator. For analysis of Cre expression, organs/tissues were harvested from PRKD1 cKO mice or floxed control mice at sacrifice and immediately flash frozen in liquid nitrogen. Organs/tissues from each mouse were homogenized in TRIzol reagent (Invitrogen) using a tissue homogenizer (VWR 200), and RNA was extracted and purified. After removal of genomic DNA contamination by treatment with DNase (DNase I, Invitrogen), samples were reverse transcribed into cDNA using the SuperScript III First-Strand Synthesis System (Invitrogen) and analyzed by qRT-PCR using Quanta SYBR Green Supermix and the Bio-Rad CFX Connect 96 Real-Time PCR Detection System. Transcript levels were normalized to the reference gene Gapdh using the ΔΔCt method as above;

primer sequences were as follows: Gapdh F: 5′-GGGAAGCCCATCACCATCTT'3′, Gapdh R: 5′-GCCTCACCCCATTTGATGTT-3′, Cre F: 5′-ACCAGCCAGCTATCAACTCG-3′, Cre R: 5′-TTACATTGGTCCAGCCACC-3′.

2.4. Alkaline Phosphatase Staining

BMMSCs were cultured for 3–10 days in osteogenic medium consisting of DMEM with 4% fetal bovine serum, 50 μM L-ascorbic acid-2-phosphate, 10 mM β-glycerophosphate and 100 nM dexamethasone with or without an initial one-day incubation with 50 ng/mL BMP2. The cells were then fixed in 75% ethanol and stained for alkaline phosphatase using One-Step™ NBT/BCIP solution (Pierce). Stained cells were scanned using an Epson Perfection 4490 Photo scanner.

2.5. Alizarin Red Staining

BMMSCs (4000 cells/well) were plated in 96-well tissue culture plates and cultured to approximately 70–80% confluence before replacing the growth medium with fresh control medium or osteogenic medium as above. The media were replaced every second day. After 2 to 3 weeks in the osteogenic medium, cells were fixed with 70% ethanol, stained with 40 mM alizarin red S (Sigma, St. Louis, MO) at pH 4.2 and photographed. The stain was solubilized using 10% cetylpyridinium chloride in 10 mM sodium phosphate, pH 7.0, and absorbance determined at 570 nM using a BioRad Microplate Manager Version 5.1 plate reader.

2.6. Generation of osteoprogenitor-specific PRKD1 cKO mice

Floxed PRKD1 mice on a mixed strain background (Flelitz et al., 2008) were obtained from Dr. Eric Olson (University of Texas Southwestern Medical Center, Dallas, TX). These mice were crossed with transgenic mice in which the osterix promoter drives Cre recombinase expression in a doxycycline-suppressible manner. Siblings were crossed to generate osteoprogenitor-specific PRKD1 cKO mice, which were then backcrossed to produce roughly 50% floxed PRKD1 controls ($PRKD1^{fl/fl}$ Osx1 Cre−) and 50% osteoprogenitor-specific PRKD1 cKO mice ($PRKD1^{fl/fl}$ Osx1 Cre+). Although the osterix-Cre transgene has been reported to cause a bone phenotype itself, at the youngest age examined (3 months) in the current studies, the skeletal phenotype of Osx1 Cre+ mice is resolved (Davey et al., 2012). After injection of calcein 2 and 6 days prior, these mice were then sacrificed at various ages and BMD and microarchitecture parameters determined as described below. Mice were genotyped using PCR of DNA isolated from tail snips performed in two reactions: one to detect the floxed PRKD1 allele and/or its recombined version and one to monitor the presence or absence of the Cre recombinase gene.

2.7. Bone Marrow Stromal Cell Isolation

Floxed and osteoprogenitor-specific PRKD1 KO mice were sacrificed and femora harvested. The ends were cut from the bones, which were centrifuged at 1300 × g for 10 min in a 1.5 mL Eppendorf tube with 100 μL Dulbecco's modified Eagles medium (DMEM) containing 10% fetal bovine serum (FBS) and 1% penicillin/streptomycin to collect bone marrow cells. These cells were plated in DMEM with 20% FBS and 1% penicillin/streptomycin/fungizone

and, after an overnight incubation, unattached cells removed by aspiration and rinsing. The attached bone marrow stromal cells were cultured for 5–6 days and RNA isolated as described above. In addition, RNA was isolated from the flushed bone shafts from the floxed or osteoprogenitor-specific conditional PRKD1 KO mice after they were frozen in liquid nitrogen and pulverized with a mortar and pestle.

2.8. DXA

Dual energy X-ray absorptiometry (DXA) of isolated femora was performed on a Lunar Piximus DXA instrument (General Electric Healthcare, Barrington, IL) as previously described (Hamrick et al., 2006).

2.9. Micro-computed tomography (μCT)

For three-dimensional (3D) bone morphometric analysis, samples were scanned using a Skyscan 1174 μCT system (Micro Photonics Inc.; PA, USA). The scan was performed at a voxel size of 15.9 μm, using a 0,25 mm aluminum filter. Bone was reconstructed using Skyscan NRecon/NRecon server software (Micro Photonics Inc.; PA, USA) with parameters standardized in all the scanned samples by the use of a single reconstruction log file. Datasets were loaded into the Skyscan CTanalyzer software (Micro Photonics Inc.; Allentown, PA) and greyscale thresholding set to a range of 70–255 for determination of 3D bone morphometric parameters, including femoral head bone mineral density (BMD), bone volume fraction (BV/TV, %), trabecular thickness (Tb.Th, mm), trabecular number (Tb.N, 1/mm), trabecular spacing (Tb.Sp, mm), and degree of anisotropy (DA). The nomenclature used is based on standards of the American Society of Bone and Mineral Research (ASBMR) for bone histomorphometric parameters. 3D images of the regions of interest were created using Skyscan CTvol software.

2.10. Dynamic Histomorphometry

A femur from each mouse was dehydrated and embedded in methyl methacrylate as previously described (McGee-Lawrence et al., 2013). Briefly, thin (5 μm) undecalcified trabecular bone sections were prepared from the distal femoral metaphysis, and dynamic histomorphometric indices were measured in the distal metaphyseal secondary spongiosa. Slides were digitized using a microscope (Olympus IX-70) and digital camera (QIcam) and analyzed using image analysis software at 200X or 400X magnification (Bioquant Osteo, Nashville TN). Single-labeled, double-labeled and mineralizing surface, as well as mineral apposition rate, were quantified from unstained sections (Dempster et al., 2013).

2.11. ELISA

Upon sacrifice blood was collected from each mouse by cardiac puncture. Serum was prepared, aliquoted and stored at −80°C until analysis. Pyridinoline cross-link (PYD) levels in serum were determined using an ELISA kit from Quidel Corp. (San Diego, CA) as per the manufacturer’s instructions.

2.12. Statistical Analysis

In vitro experiments were repeated at least 3 times with similar results. Alizarin red staining was quantified as fold change relative to GFP control cells. A log transformation on fold change was used prior to analysis. A 2 Infection (GFP vs. CRE) X 2 BMP2 (no vs. yes) ANOVA was used to determine the effect of CRE infection and treatment on osteogenic differentiation of BMMSCs. The expression of PRKD1 or PRKD2 for floxed PRKD1 and PRKD1 cKO mice was analyzed for effects due to PRKD1 cKO using a t-test on the ΔCt values [target gene (PRKD1 or PRKD2) – housekeeping gene] obtained with qRT-PCR. For *in vivo data*, DXA BMD and μCT measures (BMD, BV/TV, Tb.Th, Tb.Sp, Tb.N, DA) were analyzed using an exact Wilcoxon Rank Sum test within each age (3, 6, 9, and 12 months) to determine differences between cKO and WT mice. SAS© 9.3 (SAS Institute, Cary, NC) was used for all analysis and statistical significance was determined at $p<0.05$. Values are expressed as means ± SEM or SD as indicated and were graphed using GraphPad Prism (GraphPad, La Jolla, CA).

3. Results

3.1. Ablation of PRKD1 *in vitro*

With the assistance of the Augusta University Stem Cell Core Facility, we prepared BMMSCs from PRKD1 floxed mice obtained from Dr. Eric Olson (University of Texas Southwestern Medical Center), as described in (Flelitz et al., 2008). These cells were then infected with GFP- expressing (control) adenovirus and adenovirus expressing Cre recombinase (to delete the PRKD1 gene). Initially, we determined whether infection of BMMSCs with Cre recombinase resulted in a loss of PRKD1 mRNA and protein. BMMSCs were infected with a GFP-expressing or Cre recombinase-expressing adenovirus and incubated for 24 hours, at which time the medium was replaced and the cells incubated an additional 48 hours. The cells were then harvested and analyzed by qRT-PCR and western blotting. As shown in Figure 1A, infection with Cre recombinase resulted in a complete ablation of PRKD1 mRNA. Cells infected with GFP or Cre recombinase could be passaged; those in which the PRKD1 gene had been deleted by Cre overexpression maintained their undetectable PRKD1 levels with passaging (Figure 1B) and both transiently infected and stably deleted cells were used in subsequent experiments.

We first sought to examine the effect of loss of PRKD1 on BMMSC differentiation and mineralization *in vitro*. To do so, we infected floxed PRKD1 BMMSCs with GFP- or Cre-expressing adenovirus prior to incubating the infected cells, or uninfected control cells, in osteogenic medium as described in Methods and analyzing alkaline phosphatase (ALP) activity (differentiation) or alizarin red staining (mineralization). Although initial experiments suggested a possible slight decrease in ALP staining with Cre ablation of PRKD1, multiple experiments indicated no differences (Figure 2). On the other hand, our results showed that infection with adenovirus expressing Cre resulted in reduced alizarin red staining in comparison with GFP-expressing adenovirus (Figure 3). This effect was particularly prominent when osteogenic differentiation was enhanced by co-treating cells with BMP2, which has been reported to activate PRKD (Lemonnier et al., 2004, Celil and Campbell, 2005), upon initiation of the differentiation process with osteogenic medium. This

result suggests that PRKD1 deficiency inhibits the ability of BMMSCs to form a mineralized matrix. We would also note that these results are consistent with the finding that the presence of an allele of a dominant-negative PRKD mutant inhibits the ability of bone marrow stromal cells to differentiate as monitored by alkaline phosphatase activity and the ability to mineralize (Ford et al., 2013) but further specify that the relevant PRKD isoform is PRKD1.

3.2. Ablation of PRKD1 *in vivo*

Based on our results suggesting an involvement of PRKD1 in osteogenesis and in particular formation of a mineralized matrix by BMMSCs, we sought to investigate the effect of ablation of PRKD1 in osteoprogenitor cells on bone mineral density (BMD) and microarchitecture *in vivo*. We used the osterix-Cre transgenic mouse model in which Cre expression in osteoprogenitor cells is driven, in the absence of doxycycline, by the osterix promoter. We crossed floxed PRKD1 mice with Osx-Cre mice to generate floxed ("wild-type") and osteoprogenitor-specific PRKD1 knockout mice ("KO") and examined their bone mineral density and microarchitecture at various ages. Initially, we sought to verify PRKD1 ablation in bone cells. To do so, we harvested bone marrow stromal cells or bone shafts from floxed or KO male mice and isolated RNA from these two tissues. As shown, quantitative RT-PCR analysis of both cultured bone marrow stromal cells (Figure 4A) and bone shafts (Figure 4B) showed significantly reduced mRNA levels of PRKD1 in the cKO animals compared with the floxed control mice. PRKD2 expression was not altered (Figure 4A and B). We then measured BMD by DXA and found that at 3- and 6-months of age, osteoprogenitor-specific male PRKD1 KO mice exhibited a significant decrease in BMD of approximately 7% (Figure 5); however, by 9-months-of-age (and also subsequently at 12-months-of-age) bone appeared to be able to compensate for loss of PRKD1 such that PRKD1 KO mouse BMD was not significantly different from the floxed control at these later time points (Figure 5).

We then examined femoral microarchitecture in these male PRKD1 KO versus floxed control mice using micro-computed tomography (microCT). As illustrated in Figure 6, bone microarchitecture was affected in the 3-, 6- and 12-month-old PRKD1 cKO mice, with reduced BMD (panel A) and percentage of bone volume to total volume (panel B). In addition, we observed a significant decrease in trabecular thickness in PRKD1 cKO mouse femora at 6 and 9 months of age; the difference at 3 months did not quite achieve statistical significance (panel C). The PRKD1 cKO femora also showed a significant increase in trabecular spacing but only in the 12-month age group (Panel E). Although there appeared to be a slight decrease in trabecular number in the 3-month-old PRKD1 cKO femora (panel D), the difference did not achieve significance ($p=0.077$). There was also no significant change in the degree of anisotropy (panel F) at any age.

Using dynamic histomorphometry we also investigated the bone formation and mineralization capacity of the 3- and 6-month old osteoprogenitor-specific PRKD1 cKO and floxed control mice. We observed no difference in the single-labeled bone surface (Figure 7A), but the double-labeled surface and the mineralizing surfaces were decreased in the KO mice at both ages (Figure 7B and C). In addition, mineral apposition rate was also

significantly reduced in the PRKD1 cKO mice at 3 and 6 months of age (Figure 7D), suggesting a mineralizing defect with PRKD1 ablation in osteoprogenitor cells. Finally, we determined the effect of PRKD1 loss in osteoprogenitor cells on the bone resorption marker PYD, an indicator of type I collagen degradation, in 3- and 6-month-old PRKD1 KO and floxed control mice but detected no statistically significant differences in serum PYD levels (Figure 8).

4. Discussion

Few previous studies have examined the potential involvement of PRKD1 in bone function. Celil and Campbell (Celil and Campbell, 2005) showed in human mesenchymal stem cells that insulin-like growth factor-I (IGFI) and BMP2 activate PRKD. Using the non-selective classical protein kinase C/PRKD inhibitor Gö6976, these authors also showed the involvement of PRKD activity in mineralization as measured by alizarin red staining and ALP expression. Interestingly, they also found a role for PRKD in the induction of osterix mRNA expression by IGFI and BMP2 (Celil and Campbell, 2005), suggesting the possibility of a negative feedback effect of PRKD1 ablation on the expression of Cre recombinase driven by the osterix promoter in our mouse model. Also using the non-selective PRKD inhibitor Gö6976 in C2C12 and MC3T3-E1 osteoblastic cell lines, Westendorf and colleagues (Jensen et al., 2009) demonstrated a role for PRKD in the phosphorylation and subsequent nuclear export of histone deacetylase-7 (HDAC7), with this relocalization reversing HDAC7-mediated repression of Runx2 expression. Finally, Lemonnier et al. (Lemonnier et al., 2004) demonstrated BMP2-induced activation of PRKD in a mouse osteoblastic cell line; in these cells antisense oligonucleotide-mediated knockdown of PRKD1 reduced BMP2-elicited activation of the mitogen-activated protein kinases c-Jun N-terminal kinase (Jnk) and p38, as well as ALP activity and osteocalcin mRNA and protein expression. In addition, using both inhibitor and overexpression strategies, PRKD has been found to play a role in the osteogenic response to BMP7 and IGFI in fetal rat calvarial cells (Yeh et al., 2010). Although these studies suggested a role for PRKD in osteogenesis, most were performed *in vitro* and/or using a non-selective PRKD inhibitor in cell lines. Thus, our study is the first to show over time, that loss of PRKD1 in osteoprogenitor cells results in decreased bone mineral density, changes in bone microarchitecture and a mineralizing deficiency in mature mice.

PYD, a marker of bone resorption, was not altered in the PRKD1 cKO mice, suggesting that the low bone mass resulted from decreased bone formation rather than increased breakdown. Our *in vitro* studies provide evidence of PRKD's direct involvement in osteogenesis in BMMSCs genetically manipulated to lack PRKD1. Thus, we showed that ablation of PRKD1 using Cre recombinase in floxed PRKD1 BMMSCs inhibited mineralization induced by osteogenic medium with and without BMP2 exposure *in vitro*. In addition, in mice in which PRKD1 was targeted in osteoprogenitor cells expressing Cre recombinase under the control of the osterix promoter, reduced PRKD1 levels resulted in lower BMD as well as corresponding changes in bone microarchitecture in 3- and 6-month-old mice. These results are similar to those reported in a dominant-negative PRKD1 transgenic mouse model, in which BMD was reduced in pubertal (7- to 8-week-old) male and female mice (Ford et al., 2013). Interestingly, however, at 9 and 12 months of age, there were no significant

differences in BMD in the osteoprogenitor-specific conditional PRKD1 knockout mice, suggesting an ability of the bone to compensate for the loss of PRKD1. We have observed a similar compensatory capacity in a glucose insulinotropic polypeptide receptor knockout mouse model. In these mice, lack of the glucose insulinotropic polypeptide receptor resulted also in decreased femoral BMD at 1 and 3 months of age that normalized by 5 months (Xie et al., 2005). On the other hand, in 12-month-old mice we again observed changes in bone microarchitecture with decreased BMD and bone volume fraction at least in the femur head. We speculate that this difference may perhaps be the result of accelerated aging in the absence of PRKD1, a result that is consistent with the observed increase in trabecular spacing in the 12-month-old PRKD1 KO mice (Figure 6). Indeed, oxidative stress is known to increase with aging (reviewed in (Finkel and Holbrook, 2000)). Since in other cell types PRKD1 induces endogenous mechanisms that protect against reactive oxygen species and oxidative stress (e.g., (Storz et al., 2005, Zhang et al., 2015, Xiang et al., 2013)), this result suggests the possibility that loss of PRKD1 could result in enhanced oxidative stress to inhibit mineralization. However, this idea requires further investigation.

A limitation of our study is that our breeding scheme precluded generation of an osterix-Cre expressing control mouse (i.e., $PRKD1^{+/+}$ osx-Cre+). The osterix-Cre transgene used for conditional ablation of PRKD1 has been reported to exhibit developmental effects on bone independent of ablation of a loxP-flanked gene at younger mouse ages. Wang et al. (Wang et al., 2015) have reported craniofacial defects induced by expression of the transgene, and Davey et al. (Davey et al., 2012) reported decreased cortical bone perimeter and thickness in young mice possessing the osterix-Cre transgene (in the absence of loxp sites). These changes could be accounted for by the reduced body weight and length of these mice, and importantly, the osterix-Cre transgene-related bony changes were entirely resolved by 2–3 months of age, with no maintained differences in cortical bone expansion or accrual after this time frame (Davey et al., 2012). Therefore, despite the limitation of lacking an osterix-Cre expressing control in our studies, it seems unlikely that the differences in BMD and bone microarchitecture that we observed in the 3- and 6-month-old mice are due to the osterix-Cre transgene alone.

Li et al. (Li et al., 2017) employed a similar strategy to conditionally knock out Prkd1 in osteoprogenitor cells using the same osterix-Cre mouse model (i.e., $Prkd1^{f/f}$ Cre− or $Prkd1^{f/+}$ Cre− mice as controls, $Prkd1^{f/f}$ Cre+ mice as cKO). These authors also found a reduced bone formation phenotype in the cKO mice; however, in Li et al.'s studies the effect of the Osx-Cre transgene could have influenced outcome measures because mice were examined at only 4 and 10-weeks-of age (Li et al., 2017), at which time the skeleton is not yet fully mature (Ferguson et al., 2003) and wild-type Cre-positive animals are known to display a bone phenotype (Davey et al., 2012, Wang et al., 2015). Thus, the abnormalities detected by Li et al. (Li et al., 2017) in BMD, bone microarchitecture and bone development may have been related in part to the Cre transgene rather than PRKD1 loss. Thus, one of the previously published *in vivo* studies examined young mice in which the Cre transgene may still be exerting effects independent of the PRKD1 knockout. On the other hand, a caveat for the other was the use of a global knock-in dominant negative PKD1 allele that may also inhibit PRKD2 and was expressed in multiple bone-active tissues and investigated also in young (pubertal) mice. The results presented in the current study build upon these two

studies (Ford et al., 2013, Li et al., 2017), confirming that PRKD1 (independent of Cre transgene or PRKD2 effects) has an important role to play in osteogenesis of the mature mouse skeleton.

The mechanism(s) by which PRKD1 affects bone formation is not yet fully understood. Based on data in the literature and as mentioned above, PRKD1 might promote maintenance of mineralization by inducing endogenous antioxidant systems to detoxify reactive oxygen species generated during this process. In addition or alternatively, the ability of PRKD1 to phosphorylate and induce the relocalization of type II HDACs (reviewed in (Tao et al., 2014)) such as HDAC7 (Jensen et al., 2009) may be involved in its effects on bone formation. Other signaling molecules implicated in PRKD1's effect in bone are the Janus kinase 1 (JAK1)/signal transducer and activator of transcription-3 (STAT3) and p38 mitogen-activated protein kinase pathways: the phosphorylation (activation) status of both STAT3 and p38 was found to be decreased in differentiating calvarial osteoblasts from young PRKD1 cKO mice, although statistical analysis was not performed due to the limited number of primary cultures examined (Li et al., 2017). Finally, in endothelial cells, PRKD has been reported to phosphorylate and inactivate glycogen synthase kinase-3-beta (GSK3) (Shin et al., 2012). Inhibition of GSK3β is known to result in the stimulation of the transcriptional activity of beta-catenin by allowing its accumulation via prevention of its degradation (reviewed in (Hoeppner et al., 2009)). Since beta-catenin is a known regulator of osteogenesis (Duan and Bonewald, 2016), this interaction with the Wnt/beta-catenin pathway may underlie PRKD1's role in bone and bone formation. Clearly, further studies are needed.

Based on our results, then, PRKD1 appears to play an important role in mesenchymal stem cells *in vitro* and osteoprogenitor cells *in vivo*, contributing to the ability of these cells to form a mineralized matrix. Future studies are needed to define the exact mechanism by which PRKD1 affects bone structure and function, as well as the changes that occur with aging.

Acknowledgments

Funding: This work was supported by the National Institutes of Health [P01 AG036675 (to CMI)], including a minority supplement to LJB; WBB was supported by a VA Research Career Scientist Award. The contents of this article do not represent the views of the Department of Veterans Affairs or the United States Government.

Abbreviations

ALP	alkaline phosphatase
BMD	bone mineral density
BMMSC	bone marrow-derived mesenchymal stem cell
BMP	bone morphogenetic protein
cKO	conditional knockout
Ct	cycle threshold

DXA	dual-energy X-ray absorptiometry
IGF1	insulin-like growth factor-1
Osx	osterix
PRKD	protein kinase D
PYD	pyridinoline cross-link
qRT-PCR	quantitative reverse transcription-polymerase chain reaction
ROS	reactive oxygen species
3D	three dimensional
μCT	microcomputed tomography

References

1. Kim WK, Meliton V, Bourquard N, Hahn TJ, Parhami F. Hedgehog signaling and osteogenic differentiation in multipotent bone marrow stromal cells are inhibited by oxidative stress. J Cell Biochem. 2010; 111:1199–209. [PubMed: 20717924]
2. Bai XC, Lu D, Bai J, Zheng H, Ke ZY, Li XM, Luo SQ. Oxidative stress inhibits osteoblastic differentiation of bone cells by ERK and NF-kappaB. Biochem Biophys Res Commun. 2004; 314:197–207. [PubMed: 14715266]
3. Hamada Y, Fujii H, Fukagawa M. Role of oxidative stress in diabetic bone disorder. Bone. 2009; 45(Suppl 1):S35–8. [PubMed: 19232402]
4. Guntur AR, Le PT, Farber CR, Rosen CJ. Bioenergetics during calvarial osteoblast differentiation reflect strain differences in bone mass. Endocrinology. 2014; 155:1589–95. [PubMed: 24437492]
5. Guha S, Tanasanvimon S, Sinnett-Smith J, Rozengurt E. Role of protein kinase D signaling in pancreatic cancer. Biochem Pharmacol. 2010; 80:1946–54. [PubMed: 20621068]
6. LaValle CR, George KM, Sharlow ER, Lazo JS, Wipf P, Wang QJ. Protein kinase D as a potential new target for cancer therapy. Biochim Biophys Acta. 2010; 1806:183–92. [PubMed: 20580776]
7. Ford JJ, Yeh LC, Schmidgal EC, Thompson JF, Adamo ML, Lee JC. Protein kinase D1 is essential for bone acquisition during pubertal growth. Endocrinology. 2013; 154:4182–91. [PubMed: 23970783]
8. Yeh LC, Ma X, Matheny RW, Adamo ML, Lee JC. Protein kinase D mediates the synergistic effects of BMP-7 and IGF-I on osteoblastic cell differentiation. Growth Factors. 2010; 28:318–28. [PubMed: 20380591]
9. Jensen ED, Gopalakrishnan R, Westendorf JJ. Bone morphogenic protein 2 activates protein kinase D to regulate histone deacetylase 7 localization and repression of Runx2. J Biol Chem. 2009; 284:2225–34. [PubMed: 19029091]
10. Lemonnier J, Ghayor C, Guicheux J, Caverzasio J. Protein kinase C-independent activation of protein kinase D is involved in BMP-2-induced activation of stress mitogen-activated protein kinases JNK and p38 and osteoblastic cell differentiation. J Biol Chem. 2004; 279:259–64. [PubMed: 14573624]
11. Celil AB, Campbell PG. BMP-2 and insulin-like growth factor-I mediate Osterix (Osx) expression in human mesenchymal stem cells via the MAPK and protein kinase D signaling pathways. J Biol Chem. 2005; 280:31353–9. [PubMed: 16000303]
12. Yin DM, Huang YH, Zhu YB, Wang Y. Both the establishment and maintenance of neuronal polarity require the activity of protein kinase D in the Golgi apparatus. J Neurosci. 2008; 28:8832–43. [PubMed: 18753385]

13. Flelitz J, Kim MS, Shelton JM, Qi X, Hill JA, Richardson JA, Bassek-Duby R, Olson EN. Requirement of protein kinase D1 for pathological cardiac remodeling. Proc Natl Acad Sci USA. 2008; 105:3059–3063. [PubMed: 18287012]

14. Rodda SJ, McMahon AP. Distinct roles for Hedgehog and canonical Wnt signaling in specification, differentiation and maintenance of osteoblast progenitors. Development. 2006; 133:3231–44. [PubMed: 16854976]

15. Choudhary V, Olala LO, Kaddour-Djebbar I, Helwa I, Bollag WB. Protein kinase D1 deficiency promotes differentiation in epidermal keratinocytes. J Dermatol Sci. 2014; 76:186–95. [PubMed: 25450094]

16. Davey RA, Clarke MV, Sastra S, Skinner JP, Chiang C, Anderson PH, Zajac JD. Decreased body weight in young Osterix-Cre transgenic mice results in delayed cortical bone expansion and accrual. Transgenic Res. 2012; 21:885–93. [PubMed: 22160436]

17. Hamrick MW, Ding KH, Pennington C, Chao YJ, Wu YD, Howard B, Immel D, Borlongan C, McNeil PL, Bollag WB, Curl WW, Yu J, Isales CM. Age-related loss of muscle mass and bone strength in mice is associated with a decline in physical activity and serum leptin. Bone. 2006; 39:845–53. [PubMed: 16750436]

18. McGee-Lawrence ME, Bradley EW, Dudakovic A, Carlson SW, Ryan ZC, Kumar R, Dadsetan M, Yaszemski MJ, Chen Q, An KN, Westendorf JJ. Histone deacetylase 3 is required for maintenance of bone mass during aging. Bone. 2013; 52:296–307. [PubMed: 23085085]

19. Dempster DW, Compston JE, Drezner MK, Glorieux FH, Kanis JA, Malluche H, Meunier PJ, Ott SM, Recker RR, Parfitt AM. Standardized nomenclature, symbols, and units for bone histomorphometry: a 2012 update of the report of the ASBMR Histomorphometry Nomenclature Committee. J Bone Miner Res. 2013; 28:2–17. [PubMed: 23197339]

20. Xie D, Cheng H, Hamrick M, Zhong Q, Ding KH, Correa D, Williams S, Mulloy A, Bollag W, Bollag RJ, Runner RR, McPherson JC, Insogna K, Isales CM. Glucose-dependent insulinotropic polypeptide receptor knockout mice have altered bone turnover. Bone. 2005; 37:759–69. [PubMed: 16219496]

21. Finkel T, Holbrook NJ. Oxidants, oxidative stress and the biology of ageing. Nature. 2000; 408:239–47. [PubMed: 11089981]

22. Storz P, Doppler H, Toker A. Protein kinase D mediates mitochondrion-to-nucleus signaling and detoxification from mitochondrial reactive oxygen species. Mol Cell Biol. 2005; 25:8520–30. [PubMed: 16166634]

23. Zhang T, Sell P, Braun U, Leitges M. PKD1 protein is involved in reactive oxygen species-mediated mitochondrial depolarization in cooperation with protein kinase Cdelta (PKCdelta). J Biol Chem. 2015; 290:10472–85. [PubMed: 25759386]

24. Xiang SY, Ouyang K, Yung BS, Miyamoto S, Smrcka AV, Chen J, Heller Brown J. PLCepsilon, PKD1, and SSH1L transduce RhoA signaling to protect mitochondria from oxidative stress in the heart. Sci Signal. 2013; 6:ra108. [PubMed: 24345679]

25. Wang L, Mishina Y, Liu F. Osterix-Cre transgene causes craniofacial bone development defect. Calcif Tissue Int. 2015; 96:129–37. [PubMed: 25550101]

26. Li S, Xu W, Xing Z, Qian J, Chen L, Gu R, Guo W, Lai X, Zhao W, Li S, Wang Y, Wang QJ, Deng F. A conditional knockout mouse model reveals a critical role of PKD1 in osteoblast differentiation and bone development. Sci Rep. 2017; 7:40505. [PubMed: 28084409]

27. Ferguson VL, Ayers RA, Bateman TA, Simske SJ. Bone development and age-related bone loss in male C57BL/6J mice. Bone. 2003; 33:387–98. [PubMed: 13678781]

28. Tao H, Shi K-H, Yang J-J, Huang C, Zhan H-Y, Li J. Histone deacetylases in cardiac fibrosis: Current perspectives for therapy. Cell Signal. 2014; 26:521–527. [PubMed: 24321371]

29. Shin S, Wolgamott L, Yoon SO. Regulation of endothelial cell morphogenesis by the protein kinase D (PKD)/glycogen synthase kinase 3 (GSK3)beta pathway. Am J Physiol Cell Physiol. 2012; 303:C743–56. [PubMed: 22855295]

30. Hoeppner LH, Secreto FJ, Westendorf JJ. Wnt signaling as a therapeutic target for bone diseases. Expert Opin Ther Targets. 2009; 13:485–496. [PubMed: 19335070]

31. Duan P, Bonewald LF. The role of the wnt/beta-catenin signaling pathway in formation and maintenance of bone and teeth. Int J Biochem Cell Biol. 2016; 77:23–9. [PubMed: 27210503]

Highlights

- Loss of PRKD1 inhibits mineralization in mesenchymal stem cells (MSCs) *in vitro*.
- Loss of PRKD1 in MSCs does not affect alkaline phosphatase activity *in vitro*.
- Osteoprogenitor-specific PRKD1 loss reduces bone mineral density and mineralization.
- Osteoprogenitor-specific PRKD1 loss affects bone microarchitecture in mice *in vivo*.

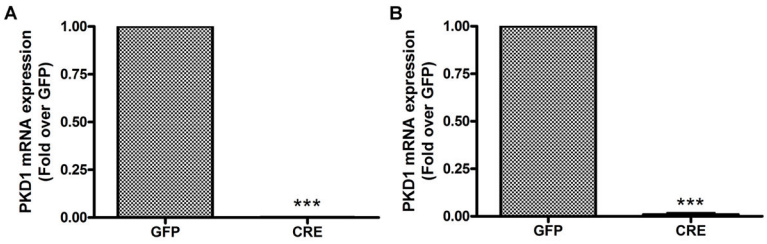

Figure 1. Adenovirus-mediated Cre recombinase expression resulted in PRKD1 loss in BMMSCs

(A) Floxed PRKD1 BMMSCs were infected with adenovirus expressing GFP (GFP) or Cre recombinase (Cre). Three days after infection PRKD1 mRNA levels were determined by qRT-PCR with GAPDH as the normalization control using the delta-delta Ct method and GFP-infected cells as the comparator. (B) Floxed PRKD1 BMMSCs were infected with adenovirus expressing GFP (GFP) or Cre recombinase (Cre). At near-confluence GFP- or Cre-expressing BMMSCs were passaged to generate stable cell lines. PRKD1 mRNA levels were determined in the passaged cells by qRT-PCR with GAPDH as the normalization control using the delta-delta Ct method and GFP-infected cells as the comparator.

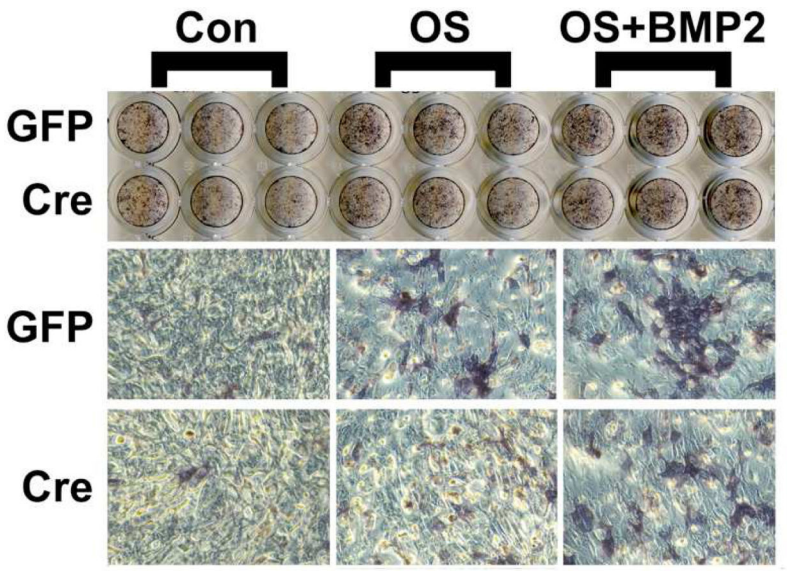

Figure 2. PRKD1 loss in BMMSCs has little effect on alkaline phosphatase activity *in vitro*

Floxed BMMSCs were infected with adenovirus expressing GFP or Cre (or uninfected) as in Figure 1. The cells were then treated for 10 days with control medium (containing 2% FBS) or osteogenesis-stimulating (OS) medium containing dexamethasone, β-glycerophosphate and ascorbic acid in the presence and absence of 50 ng/mL BMP2 (added for the first 48 hours only), and alkaline phosphatase staining determined. Shown is a representative of 3 experiments.

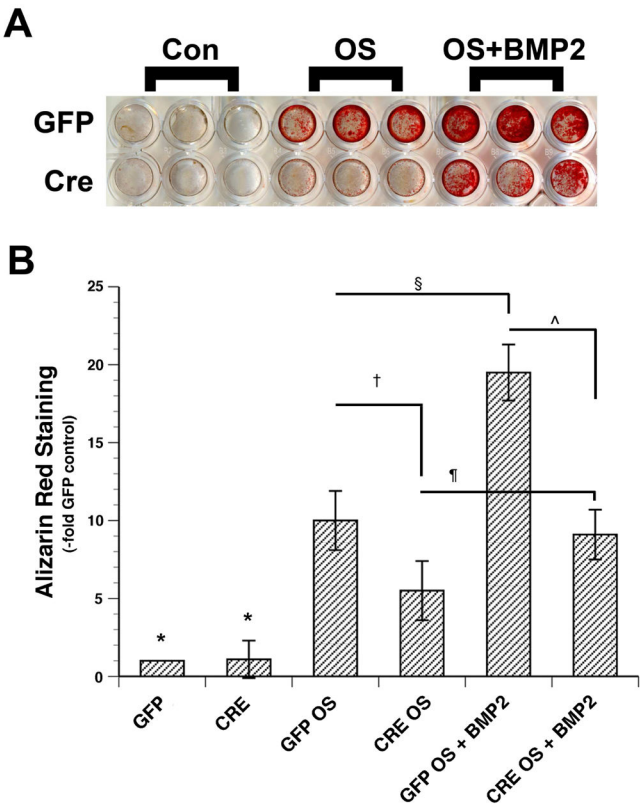

Figure 3. PRKD1 loss in BMMSCs inhibits mineralization *in vitro*

Floxed PRKD1 treated as in Figure 1 were cultured for 18–25 days and alizarin red staining determined. (A) Shown is a representative experiment. (B) Cumulative results from 3 separate experiments expressed as the percent maximal response are shown as means ± SEM; *p<0.05 versus all OS and OS + BMP2 conditions; †, ¶, ¥, p<0.05 as indicated.

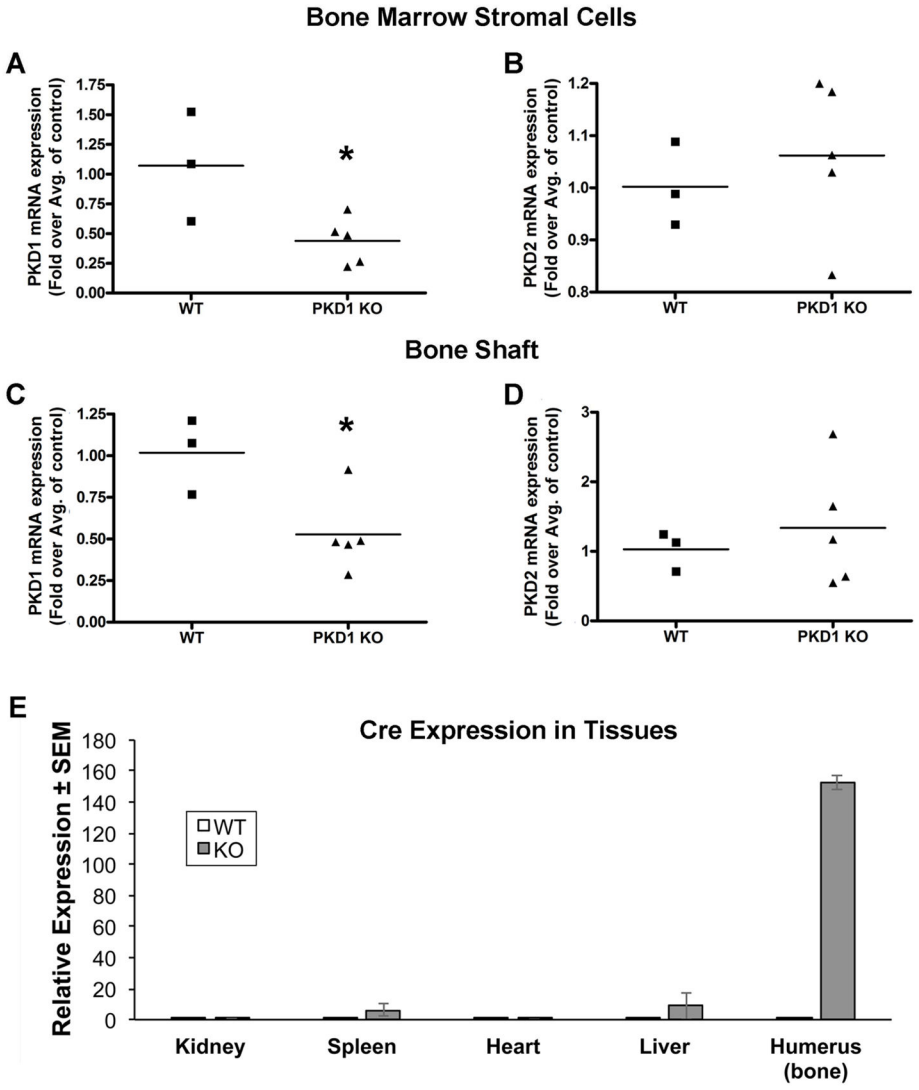

Figure 4. Bone marrow stromal cells and bone from osteoprogenitor-specific conditional PRKD1 knock-out mice show reduced expression of PRKD1, but not PRKD2

Floxed PRKD1 mice were crossed with a transgenic mouse model in which the doxycycline-regulated osterix promoter drives Cre expression. (A and B) Adherent bone marrow cells were isolated from floxed and conditional PRKD1 knockout femora and (A) PRKD1 and (B) PRKD2 expression measured by qRT-PCR. (C and D) RNA was also isolated from bone shaft and (C) PRKD1 and (D) PRKD2 expression monitored by qRT-PCR. Each symbol represents an individual mouse; the line denotes the mean fold expression relative to the average control value. (E) Tissue-specific Cre expression was demonstrated by measuring Cre mRNA levels in kidney, spleen, heart and relative to bone using qRT-PCR with Gapdh as the normalization control in the osteoprogenitor-specific PRKD1 KO and floxed control mice. Results represent the means ± SEM of 3–4 individual 3-month-old male mice.

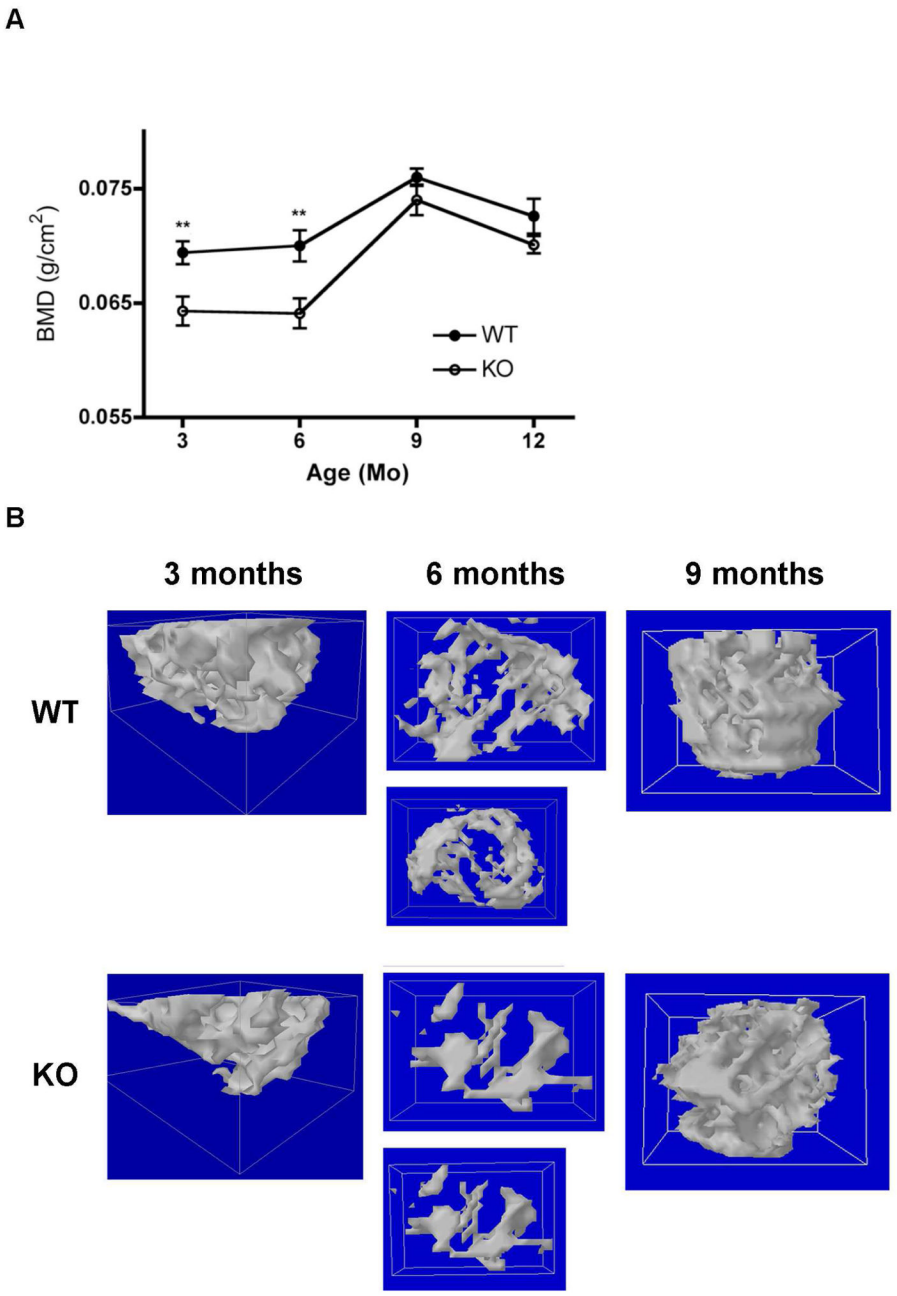

Figure 5. Conditional PRKD1 knockout mice show reductions in BMD as well as changes in bone microarchitecture at 3 and 6 months of age

(A) Conditional PRKD1 knockout mice ("KO") and floxed littermates ("WT") at various ages were sacrificed, the femora removed and bone mineral density (BMD) determined by DXA as described in Methods (floxed n=10–13, cKO n=10–13);*p<0.05, **p<0.01. (B) The femoral heads of floxed ("WT") and cKO ("KO") mice of various ages were analyzed by microCT (floxed n=10–13, cKO n=10–13). Two mice of the 3-, 6- and 9-month-old age groups (one WT and one PRKD1 knockout) were randomly selected and 3-dimensional reconstruction images prepared as described in Methods.

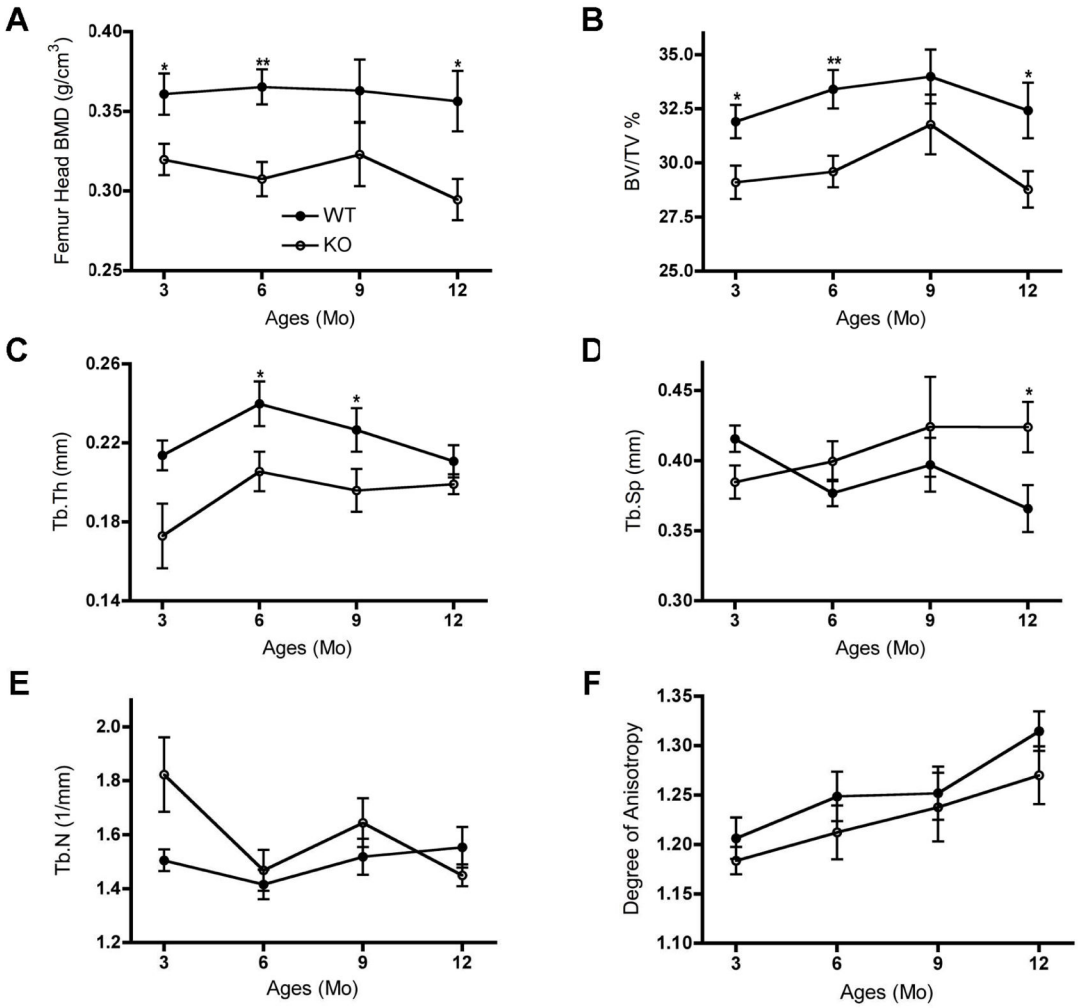

Figure 6. PRKD1 ablation in osteoprogenitor cells of conditional PRKD1 knockout mice affects the microarchitecture of bone

The femoral heads of 3-, 6-, 9- and 12-month-old floxed (“WT”) and cKO (“KO”) mice were analyzed by microCT (floxed n=10–13, cKO n=10–13). Mean ± SD values are shown for various bone parameters (TV = total volume; BV = bone volume; Tb.Th = trabecular thickness; Tb.N = trabecular number; Tb.Sp = trabecular spacing); *p<0.05, **p<0.01.

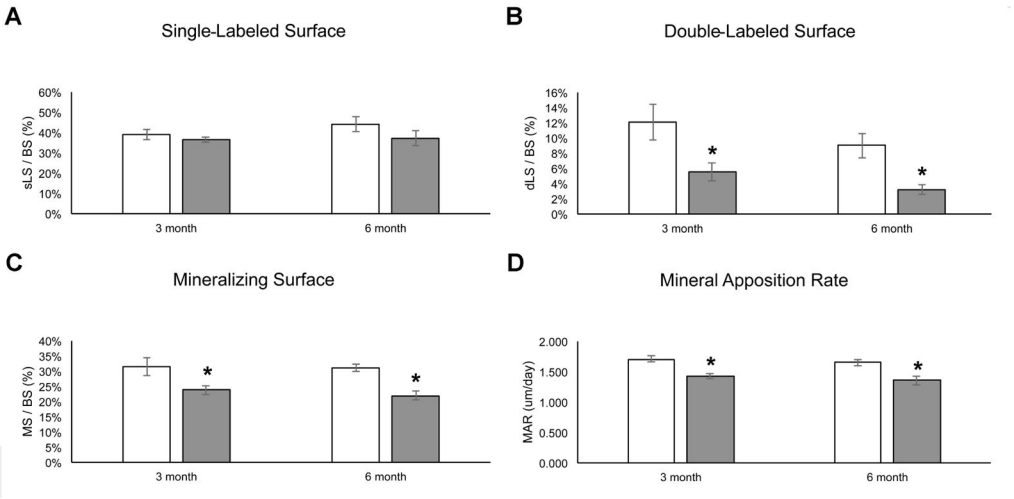

Figure 7. PRKD1 ablation in osteoprogenitor cells of conditional PRKD1 knockout mice reduces the mineralizing capacity of bone

Conditional PRKD1 knockout mice (filled bars) and floxed littermates (open bars) at 3 and 6 months of age were sacrificed, the femora removed and (A) single-labeled bone surface, (B) double-labeled bone surface, (C) mineralizing surface and (D) mineral apposition rate determined by dynamic histomorphometry as described in Methods (floxed n=10–13, cKO n=10–13);*$p<0.05$.

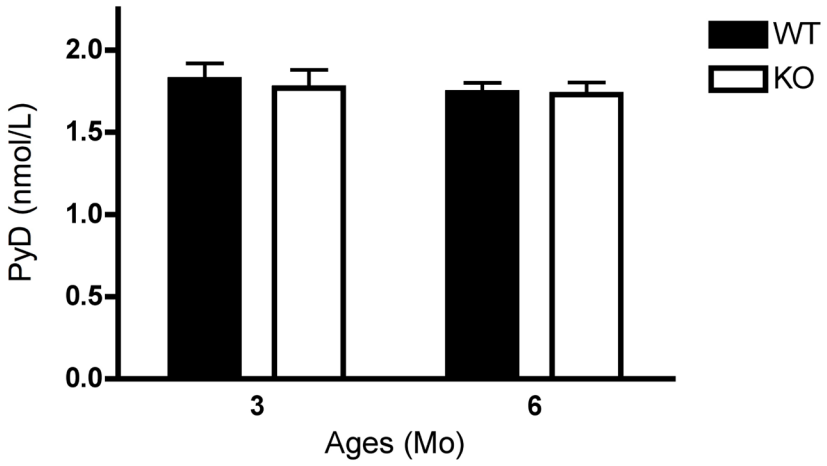

Figure 8. PRKD1 ablation has no effect on serum PYD levels in 3- or 6-month-old osteoprogenitor-specific conditional PRKD1 knockout mice

Serum from blood collected by cardiac puncture from floxed (“WT”) or cKO (“KO”) mice upon sacrifice was assayed using an ELISA kit for PYD levels. Results represent the means ± SD of 10–13 mice per age group and genotype.